Supplementary Information (SI) for Journal of Materials Chemistry C.
This journal is © The Royal Society of Chemistry 2024

Supporting Information

Dopant-free Tert-butyl Zn (II) Phthalocyanines: Impact of Substitution on Photo-Physical Properties in Their Role in Perovskite Solar Cells

Mahdi Gassara, [a†] José Garcés-Garcés,[b†] Luis Lezama,[c] Javier Ortiz,[b] Fernando Fernández-Lázaro,[b] Samrana Kazim,[a,d,e] Ángela Sastre-Santos,[b*] Shahzada Ahmad [a,e*]

[a]BCMaterials, Basque Center for Materials, Applications, and Nanostructures, UPV/EHU Science Park, 48940, Leioa, Spain, Email: shahzada.ahmad@bcmaterials.net

[b]Área de Química Orgánica, Instituto de Bioingeniería, Universidad Miguel Hernández, Avda. Universidad S/N, 03202, Elche, Spain. Email: asastre@umh.es

[c]Departamento de Química Inorgánica, Facultad de Ciencia y Tecnología, Universidad del País Vasco, UPV/EHU, Sarriena s/n, 48940, Leioa, Spain

[d]Materials Physics Center, CSIC-UPV/EHU, Paseo Manuel de Lardizabal 5, 20018, Donostia - San Sebastian, Spain

[e]IKERBASQUE, Basque Foundation for Science, Bilbao, 48009, Spain

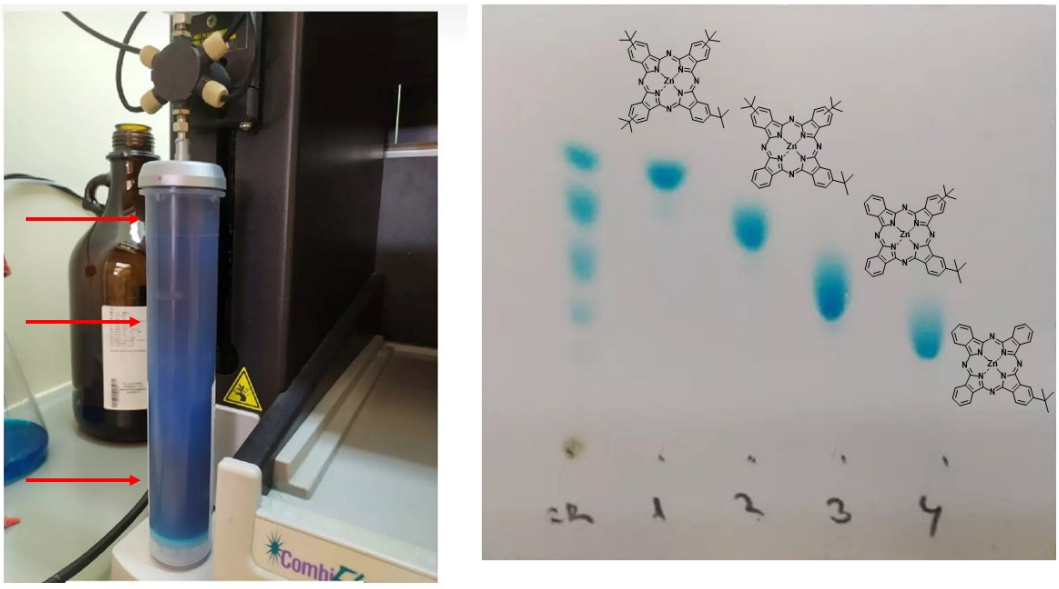

Figure S1. a) ZnPcs 1-4 bands in the chromatography column; b) TLC plate showing the reaction crude *vs* the different pure fractions of **ZnPcs 1-4** in a 5/6 ratio 3:1.

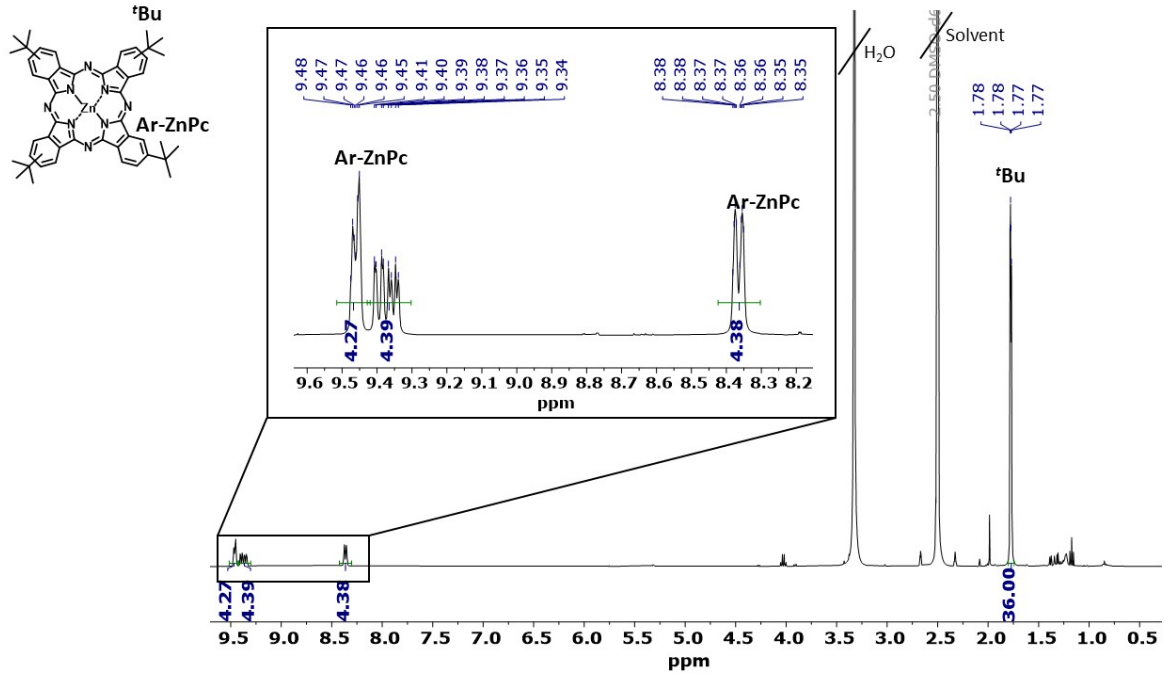

Figure S2. ^{1}H-NMR spectrum of ZnPc-1 in DMSO-d_6 (400 MHz, 25 ^{o}C).

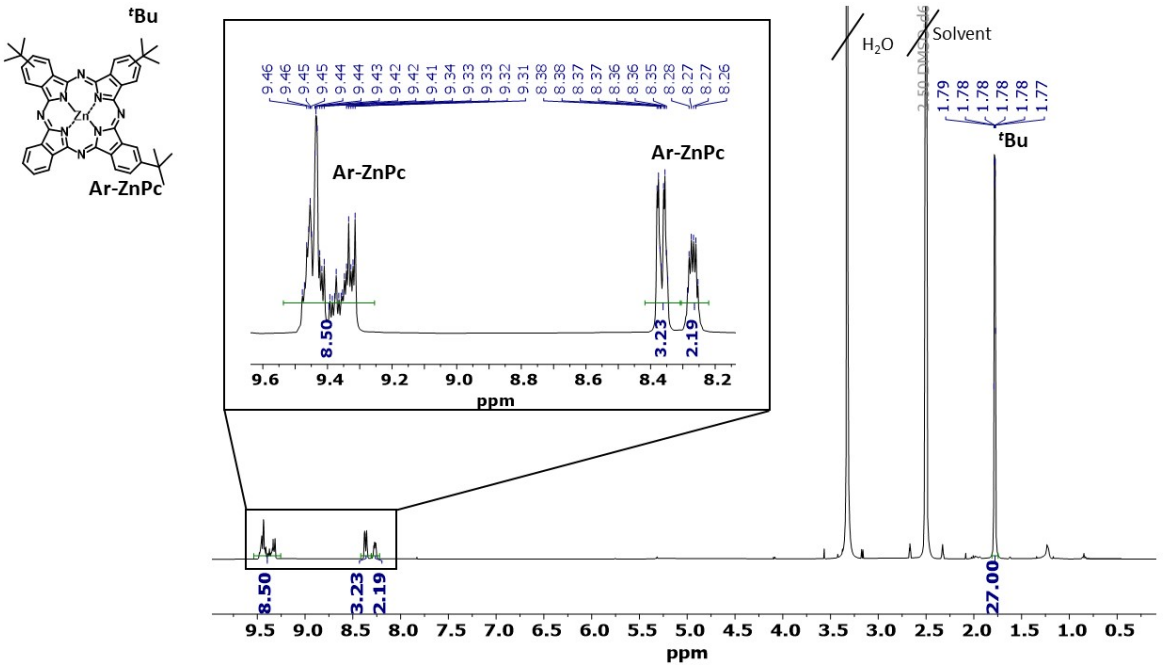

Figure S3. ^{1}H-NMR spectrum of ZnPc-2 in DMSO-d_6 (400 MHz, 25 ^{o}C).

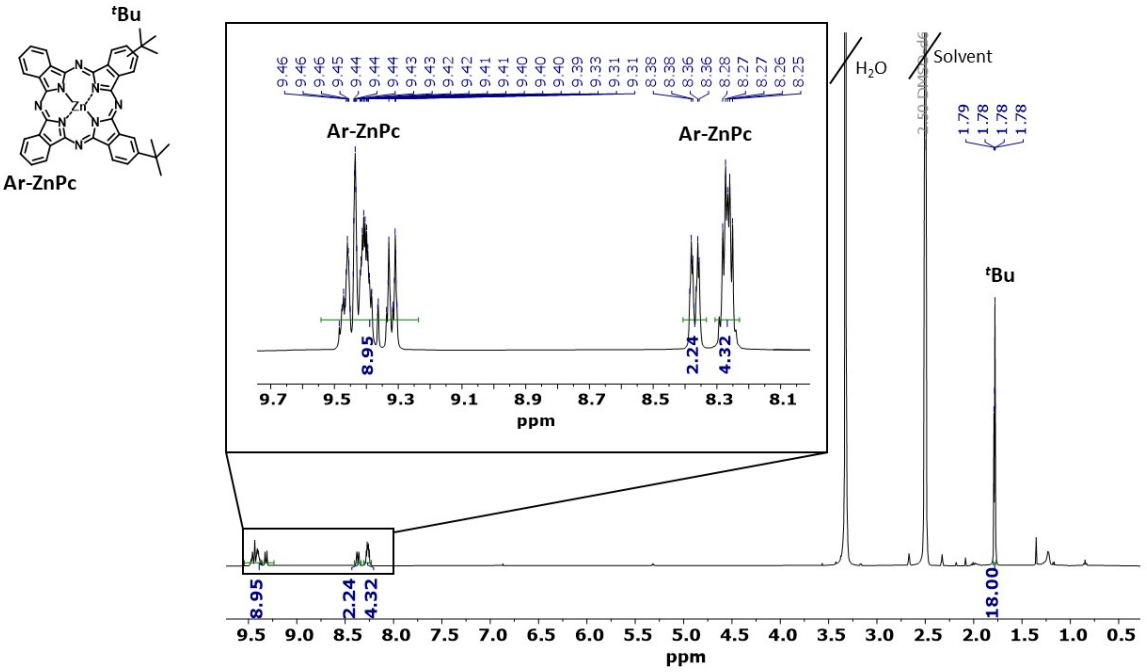

Figure S4. ^{1}H-NMR spectrum of ZnPc-3 in DMSO-d_6 (400 MHz, 25 ^{o}C).

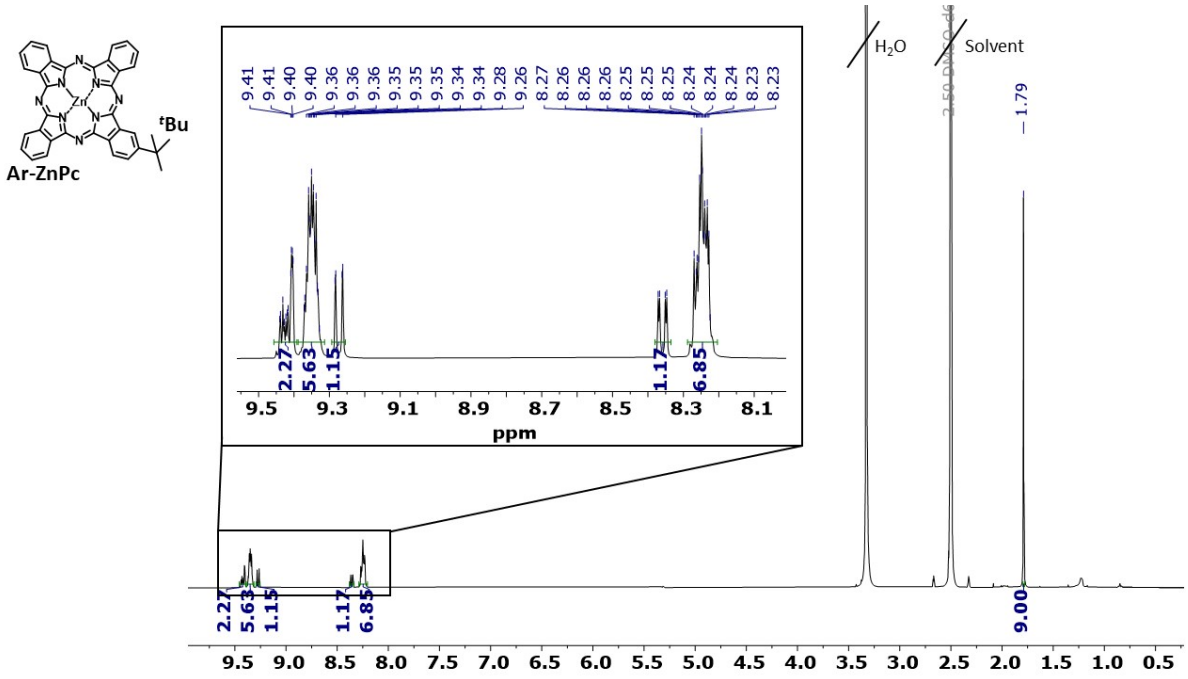

Figure S5. ^{1}H-NMR spectrum of ZnPc-4 in DMSO-d_6 (400 MHz, 25 ^{o}C).

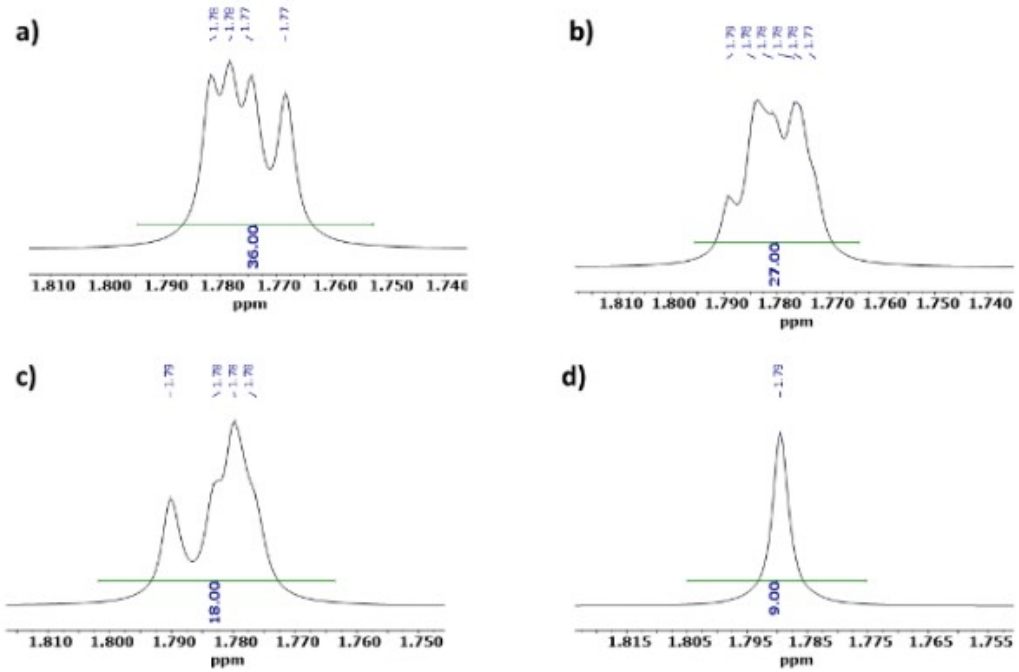

Figure S6. ^{1}H-NMR aliphatic region (DMSO-d_6, 25 °C) of a) **ZnPc-1**, b) **ZnPc-2**, c) **ZnPc-3**, and d) **ZnPc-4**.

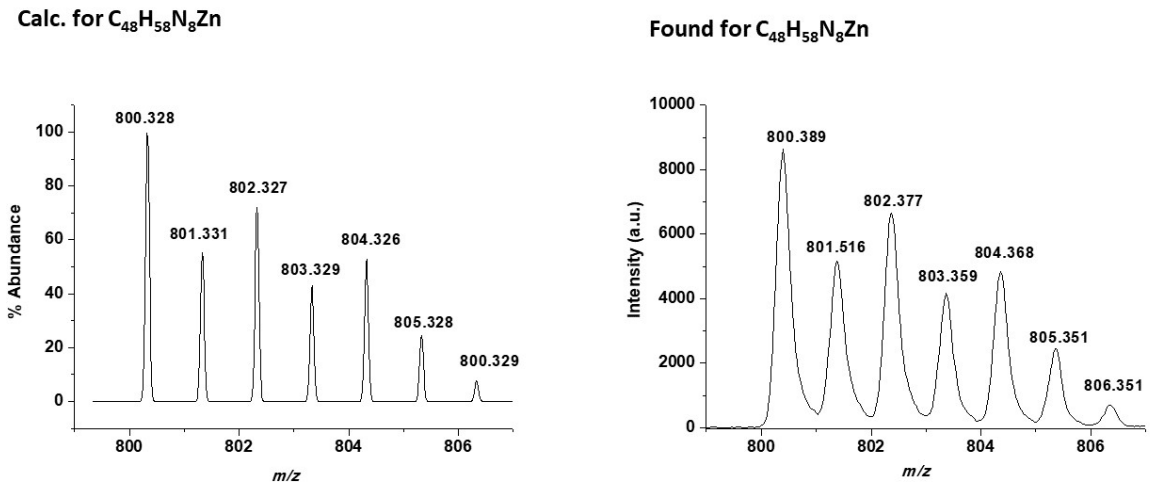

Figure S7. HR MALDI-ToF spectrum of ZnPc-1.

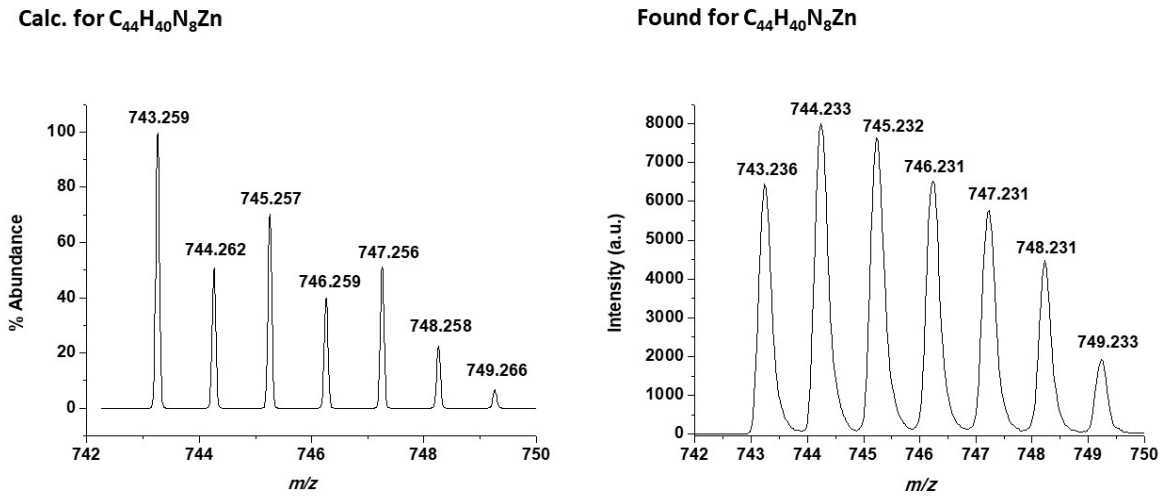

Figure S8. HR MALDI-ToF spectrum of ZnPc-2.

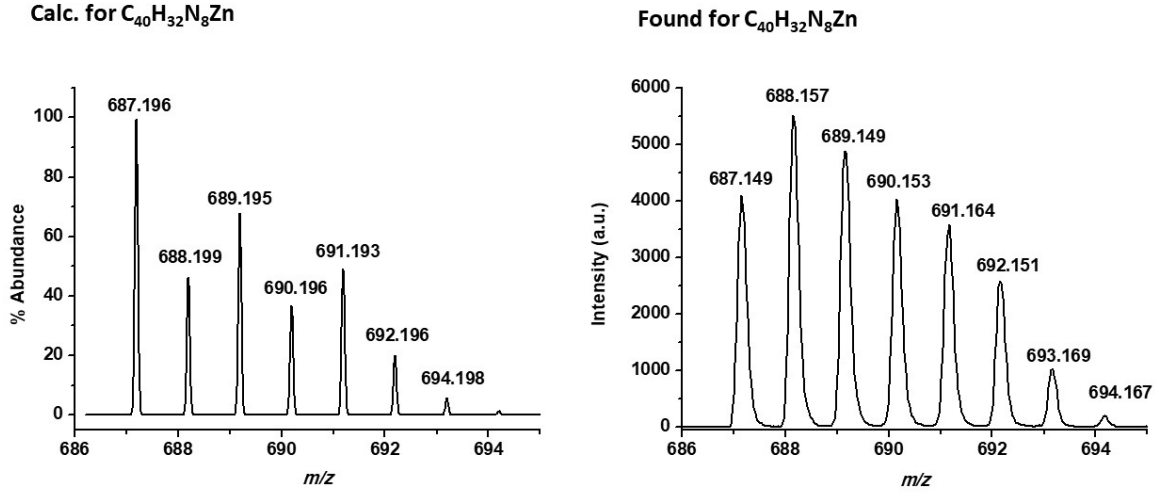

Figure S9. HR MALDI-ToF spectrum of ZnPc-3.

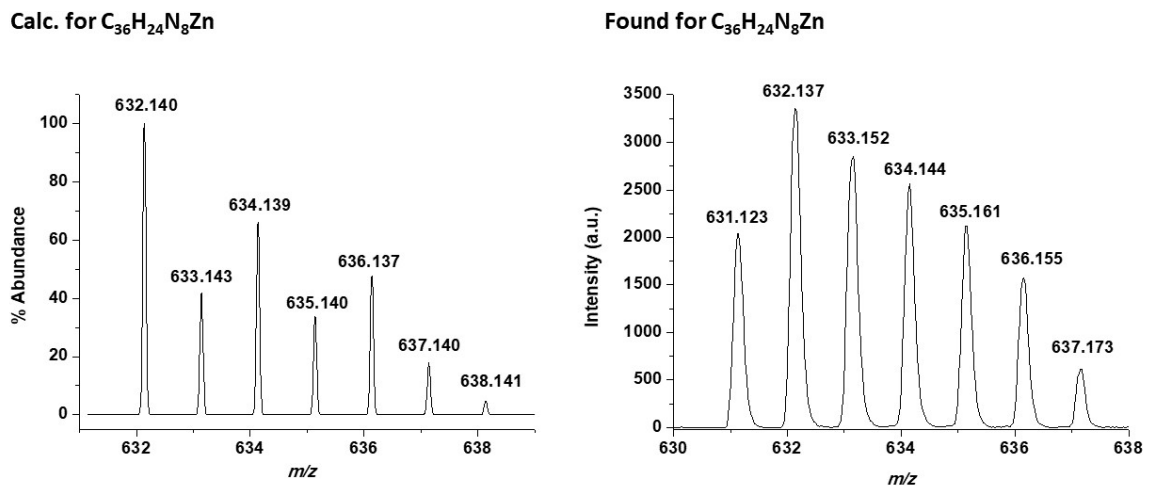

Figure S10. HR MALDI-ToF spectrum of ZnPc-4.

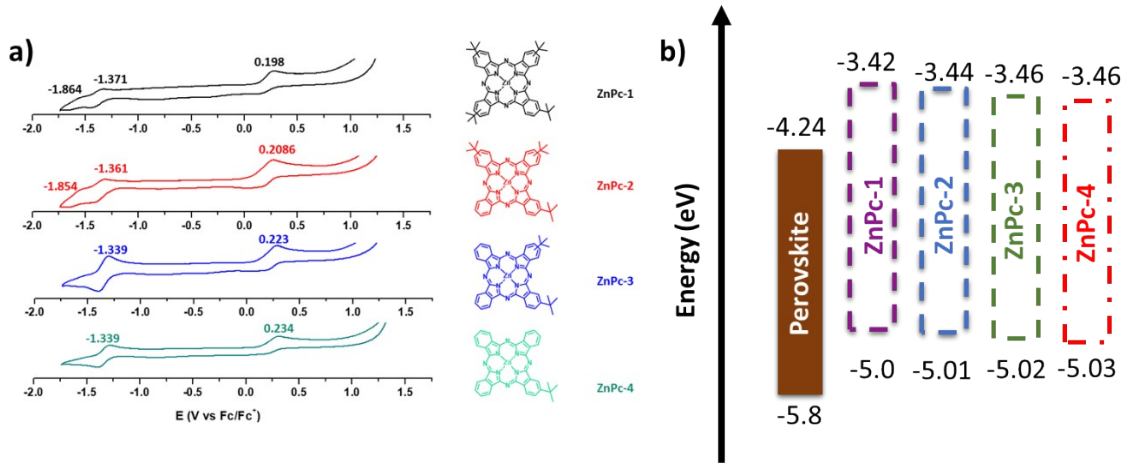

Figure S11. a) Cyclic voltammogram of ZnPcs (DMF, 25 ºC), and b) energy level band diagram of ZnPc HTMs and perovskite.

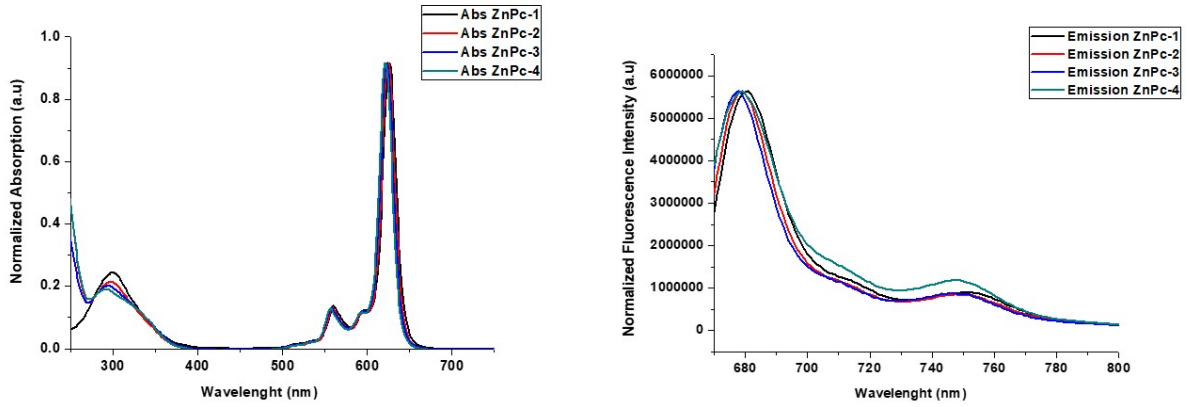

Figure S12. UV-vis and emission in $CHCl_3$ solution of the ZnPcs 1-4.

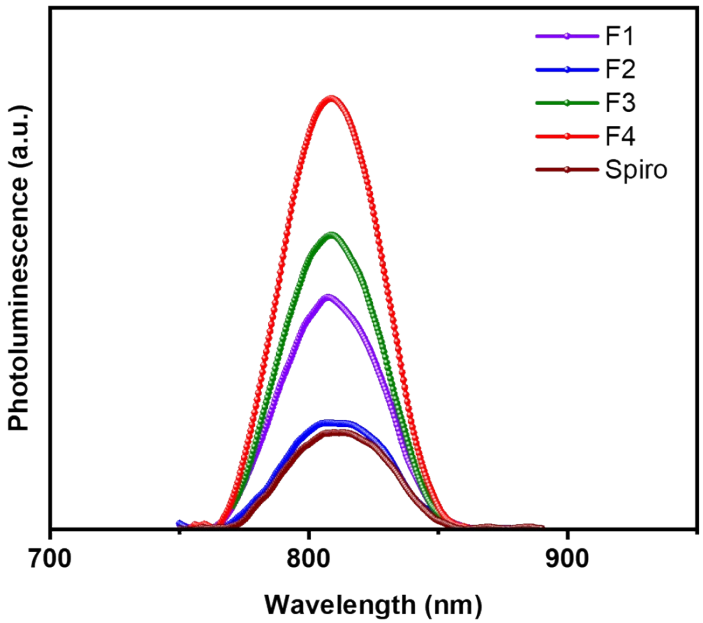

Figure S13: ss-PL spectra of perovskite with HTMs (Spiro, ZnPc-1, ZnPc-2, ZnPc-3, and ZnPc-4) thin films.

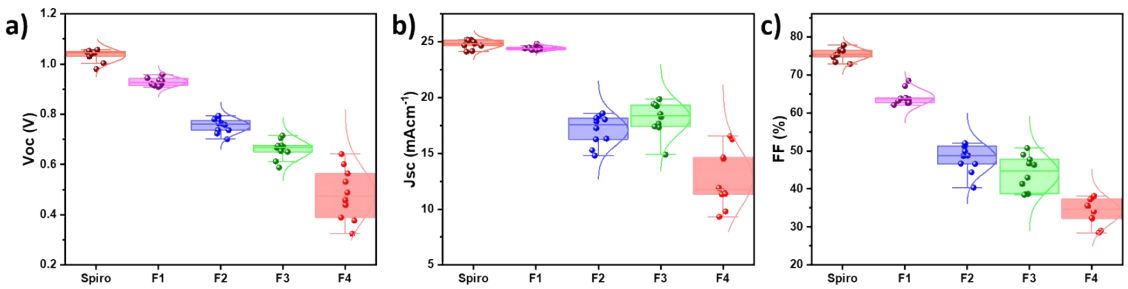

Figure S14: Statistical data of device parameters for a) V_{OC}, b) J_{SC}, and c) Fill factor.

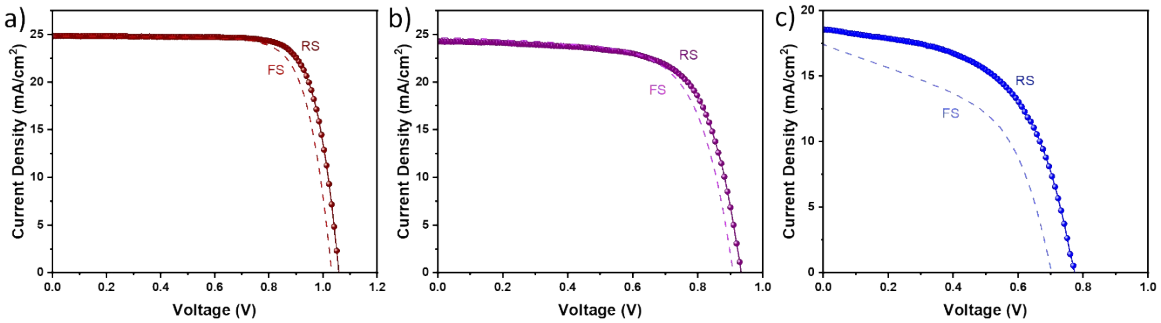

Figure S15. Reverse and forward scan *J-V* curves for PSCs based on a) ZnPc -1, b) ZnPc-2, and Spiro-OMeTAD.

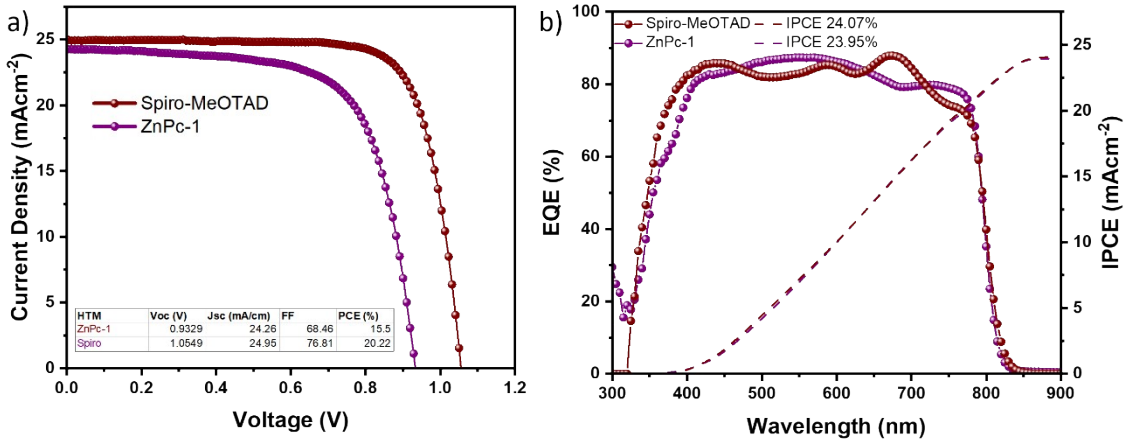

Figure S16. *J-V*, EQE, and IPCE curves of the reference and ZnPc-1.

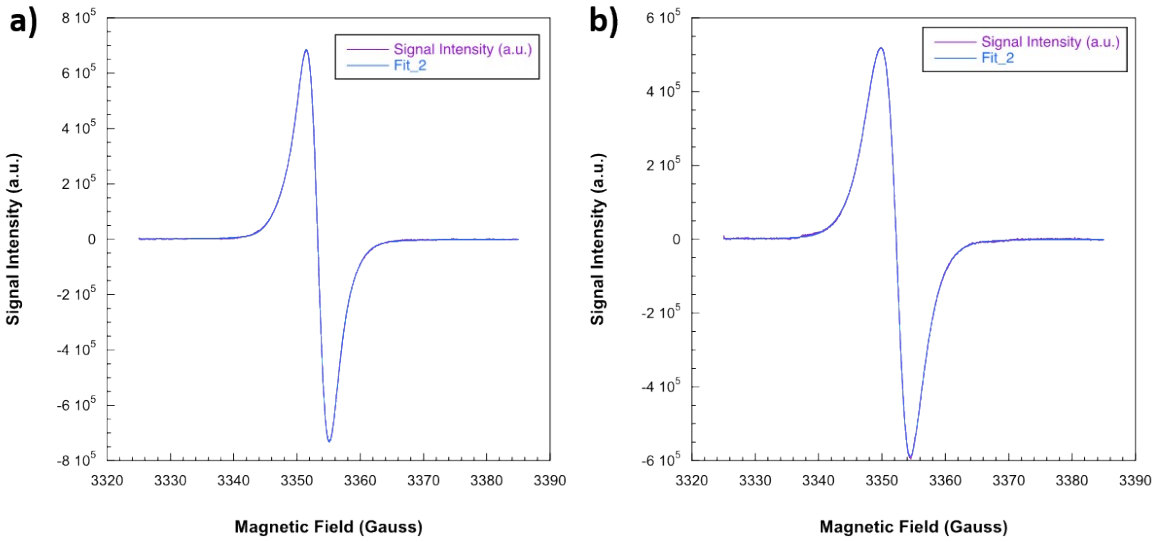

Figure S17. X-band EPR spectra recorded on solid samples of a) ZnPc-1, and b) ZnPc-2.

Table S1. Calculated values of conductivity and hole mobility data of ZnPc HTMs.

HTM	Conductivity (S/cm)	Mobility (cm^2/Vs)
ZnPc-1	2.0×10^{-6}	1.07×10^{-5}
ZnPc-2	1.95×10^{-6}	6.97×10^{-6}
ZnPc-3	2.82×10^{-6}	1.35×10^{-5}
ZnPc-4	2.08×10^{-6}	3.8×10^{-6}

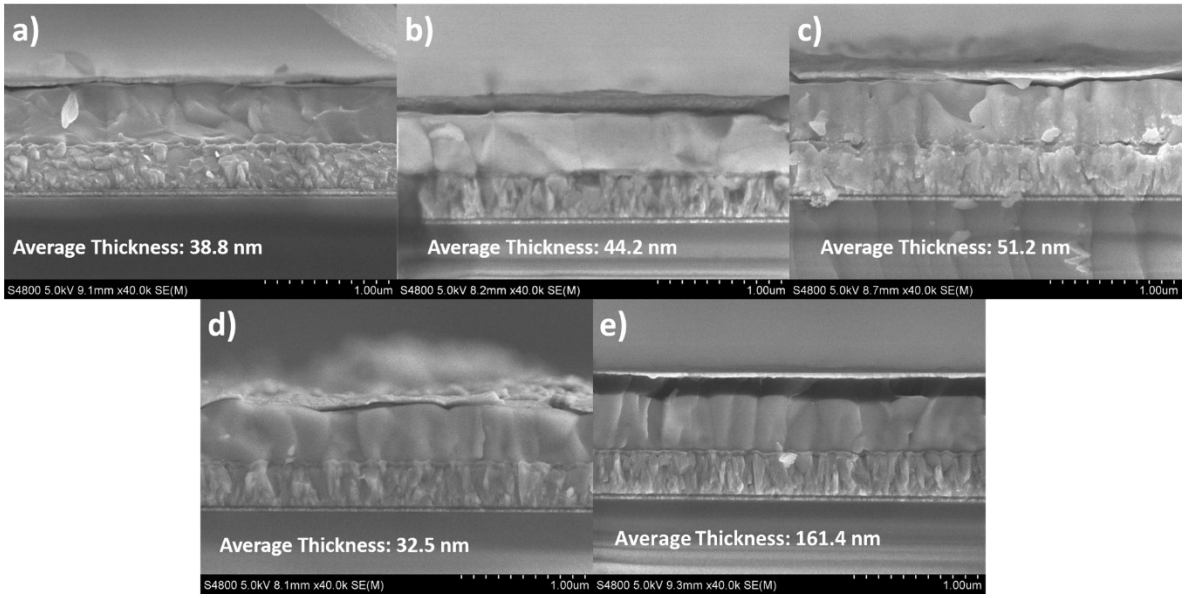

Figure S18. Cross-sectional SEM images of FTO/b-TiO_2/SnO_2/Perovskite/HTM/Au devices and average thickness for a) ZnPc-1, b) ZnPc-2, c) ZnPc-3, d) ZnPc-4, and e) Spiro-OMeTAD.

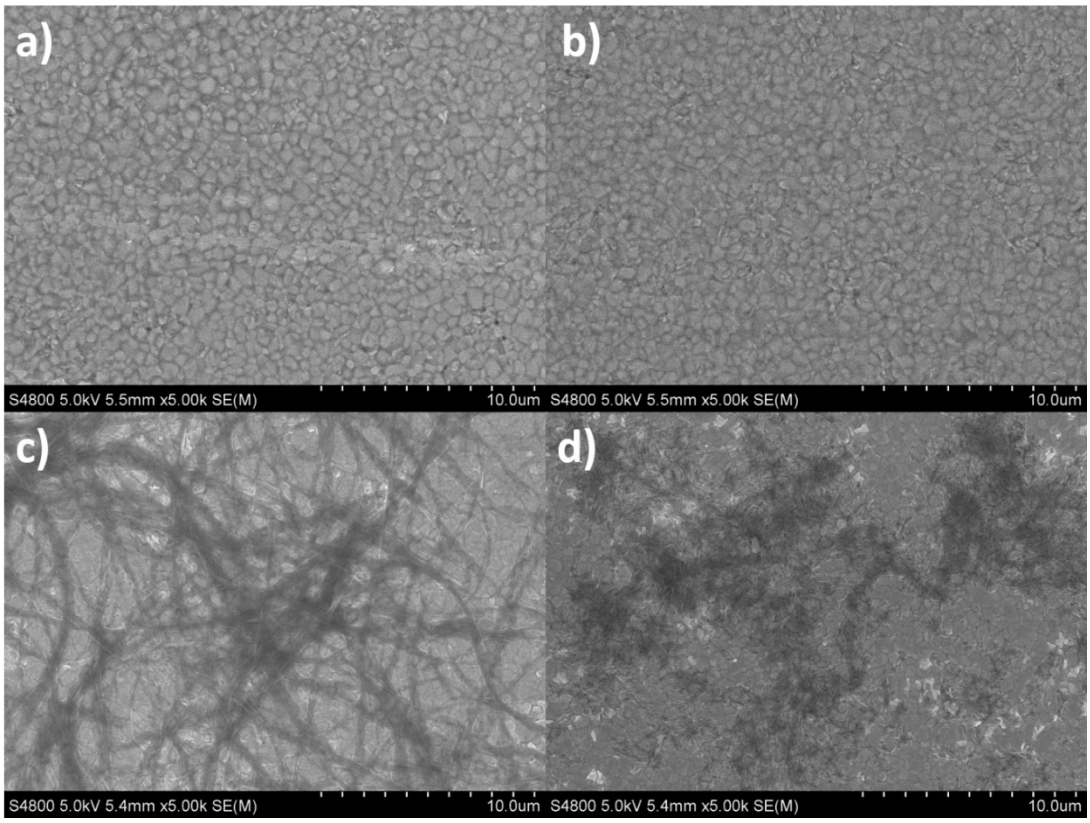

Figure S19. SEM surface image at 10 μm scale for a) ZnPc-1, b) ZnPc-2, c) ZnPc-3, and d) ZnPc-4.

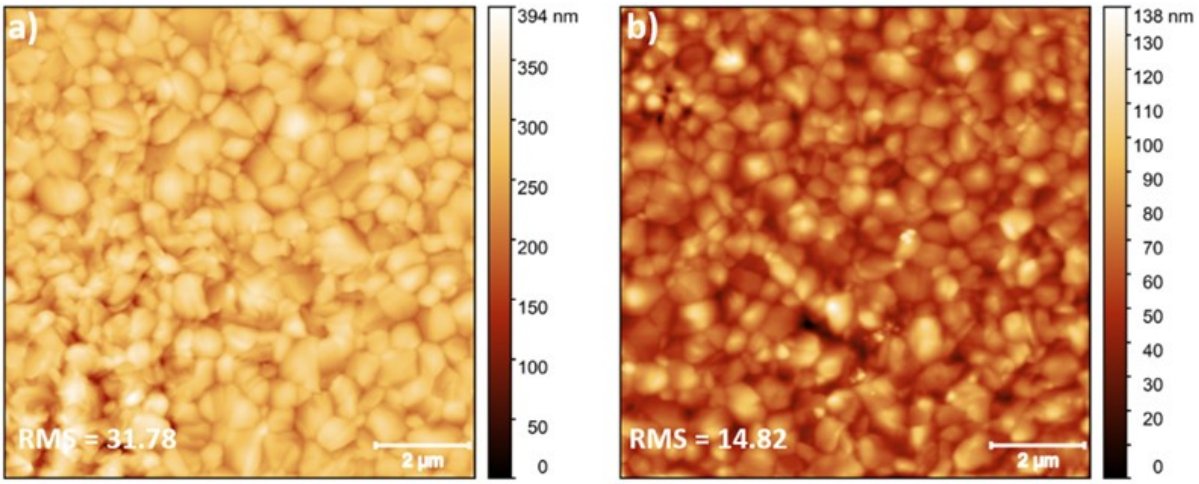

Figure S20. Scanning probe microscopy (SPM) images of a) pristine perovskite and b) perovskite/ZnPc-1.

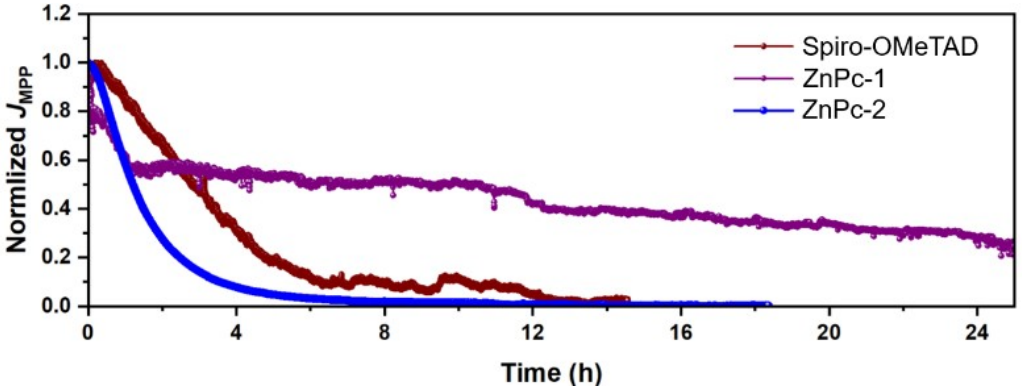

Figure S21. The normalized current density of continuous maximum power point tracking (MPP) for unencapsulated with Spiro-OMeTAD, ZnPc-1, and ZnPc-2 HTMs under ambient conditions (RH 55-65%, 310k).